

Axially Loaded Grouted Connections in Fatigue Tests

Peter Schaumann¹, Alexander Raba¹ and Anne Bechtel¹

1: Institute for Steel Construction, Leibniz Universität Hannover, Germany

Grouted Connections are a common joining technique for substructures of offshore wind turbines. Nevertheless, at present insufficient knowledge is available for the fatigue behaviour of grouted connections having a large grout annulus and being installed in submerged ambient conditions. This paper presents results from small- and large-scale fatigue tests of grouted connections. The small-scale tests reveal a significant impact of the surrounding water. The large-scale tests indicate that a larger grout annulus influences the fatigue behaviour significantly by provoking a stiffness degradation.

Keywords: Grouted Connection, Jacket, Support Structure, Fatigue, Submerged

1 Introduction

Until the year 2030, up to 40 new offshore wind farms have to be built to reach the goals of the German government [1] for the transformation of Germany's electric power supply system. This corresponds to roughly 3'000 new offshore wind turbines (OWT) mainly located in the German Exclusive Economic Zone (EEZ) of the North Sea. According to the Maritime Spatial Plan [2], most of the designated farm areas are located in water depths of 30 m and deeper. One possible substructure for these water depths is the jacket (cf. Figure 1).

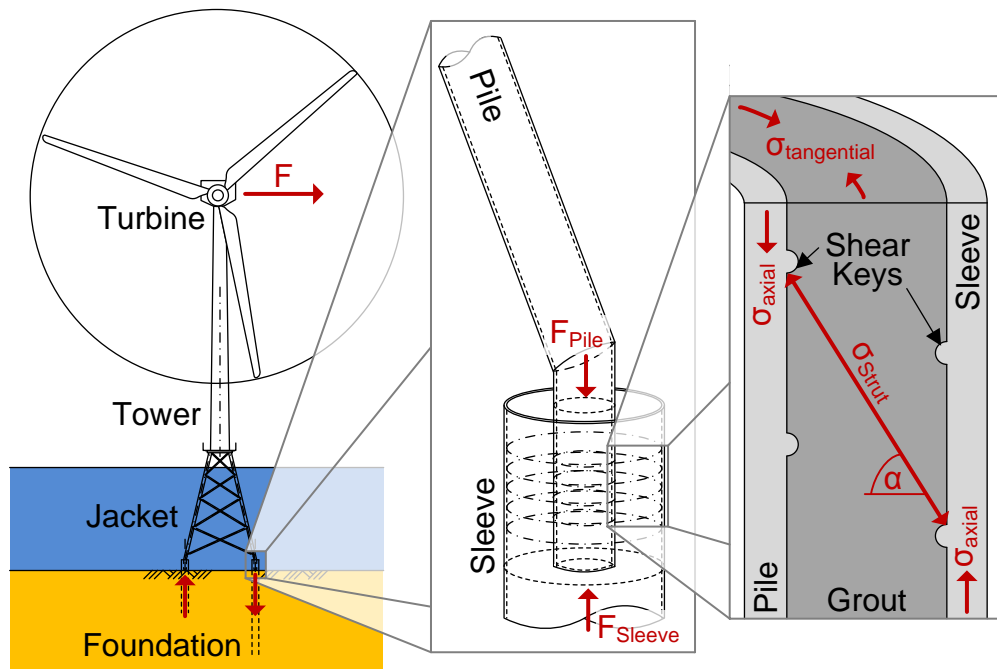


Figure 1: Grouted joint in a jacket substructure for OWTs, detail of grouted joint and load bearing behaviour

The foundation of a jacket consists of steel tubes driven into the seabed. Into these tubes (sleeves) the jacket legs (piles) are placed and the resulting annuli are filled with a high performance grout material (cf. Figure 1). For a defined interlocking between steel and grout, weld beads (shear keys) are applied to the facing steel surfaces. This joining technique is known as grouted connection and has been widely utilized in the offshore oil and gas industry.

Due to the jacket's structure, dead loads as well as alternating loads from wind and wave are split into predominantly axial force couples that are transferred through the grouted connections

into the foundation. Within the grouted connection the loads are transferred from pile to sleeve via compression struts that occur between opposing shear keys and tangential stresses in the surrounding steel tubes (cf. Figure 1).

Compared to grouted connections used in the oil and gas industry, grouted connections of jacket substructures in OWTs have larger dimensions, a significantly larger grout layer thickness and are exposed to loads which are dominated by wind and wave actions. Moreover, the currently used grout materials have much higher strengths compared to the ones used for the oil and gas platforms. Consequently, knowledge and experiences from the oil and gas industry have to be verified and extended to become applicable for the current design of OWT grouted connections. Furthermore, the grouted connections of jackets are located at seabed level being fully submerged. This particular boundary condition has been neglected in prior experimental investigations on grouted connections.

The research project 'Grouted Joints for Offshore Wind Energy Converters under reversed axial loadings and upscaled thicknesses – GROWup' (funding sign 0325290) deals with the fatigue behaviour and execution perspectives of grouted connections in jackets. At the Institute for Steel Construction, Leibniz Universität Hannover the fatigue behaviour of small and large-scale grouted connection specimens is investigated. In this paper results of the conducted tests are presented.

2 Small-scale tests

To investigate various parameters at an economic level, a small-scale grouted connection specimen (cf. Figure 2, left) was developed [3]. The specimen consists of comparatively thick steel tubes to exclude a failure of the steel components. Rectangular shaped shear keys are turned out of the steel surfaces. Due to the compact steel tubes, the specimen's flexibility is not comparable to grouted connections in real structures. Nevertheless, the test specimens account for a realistically multiaxial stress state in the grout section. As filling materials two industrial high performance grouts with a low strength of $f_{cu} = 90 \text{ N/mm}^2$ and a high strength of $f_{cu} = 140 \text{ N/mm}^2$ are investigated.

After production of a batch of specimens and 28 days of curing in a water basin, their static resistance F_{ULS} is determined. Therefore, three specimens are compressed in a displacement controlled test with a load application speed of 0.2 mm/min. The average F_{ULS} of the three specimens represents the static capacity of the batch and is used as a reference value for the subsequent fatigue tests.

The fatigue tests are conducted in a force controlled test rig (cf. Figure 2, right) with a maximum compressive load of $F_{max} = 0.5 F_{ULS}$ and a minimum compressive load of

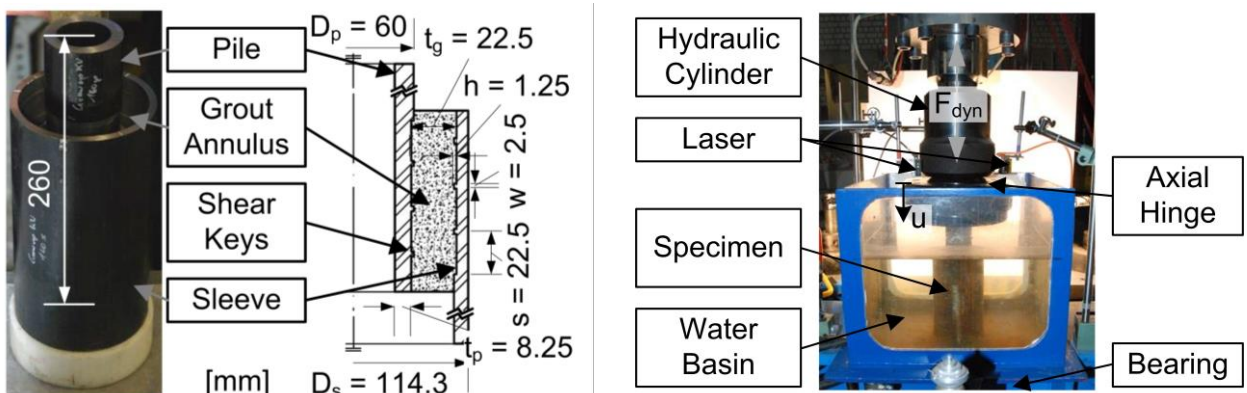


Figure 2: Geometry of small-scale specimens (left) and test rig for the small-scale fatigue tests (right)

$F_{\min} = 0.05 F_{\max}$. This relation corresponds to $R = 20$. During each test, the load level and the loading frequency are kept constant. Applied force F and relative displacement of the specimen are recorded and the number of applied load cycles is determined. With the help of a water basin, the ambient conditions (AC) dry and wet are investigated in the tests, where wet means a fully submerged grout section.

Figure 3, top left, shows the force displacement behaviour of test specimens under quasi static compression. The behaviour can be separated into three stages. Up to about 50 % F_{ULS} (cf. P1) the connection shows a linear elastic behaviour. Then the first cracks due to tensile stresses transverse to the compression struts occur and cause a stiffness reduction in stage 2. Finally, the static resistance F_{ULS} is reached at P3 and afterwards the displacement increases while the bearable load reduces in stage 3. According to observations by Schaumann et al. (cf. [4] and [5]) loading small-scale specimens up to 50 % of their static capacity will cause no significant damage within the grout section.

This conclusion corresponds to the results of the small-scale fatigue tests achieved under dry AC and shown in Figure 3, top right as gray diamonds. All six specimens reached the test termination criterion of 2 million load cycles and showed no significant degradation. In comparison to that, specimens tested under the same loading conditions but in wet AC failed at about 50.000 load cycles. Besides the individual test results, the blue boxes in Figure 3, top right indicate the 95 % confidence interval (CI) and the mean value differentiated by the material. The overlapping confidence intervals show that no significant difference between the two grout materials, regarding their fatigue behaviour could be detected. Overall, the shown fatigue behaviour alludes that water introduces new damage mechanisms to the connection.

Since real grouted connections are mainly loaded with a frequency of about 0.3 Hz, further

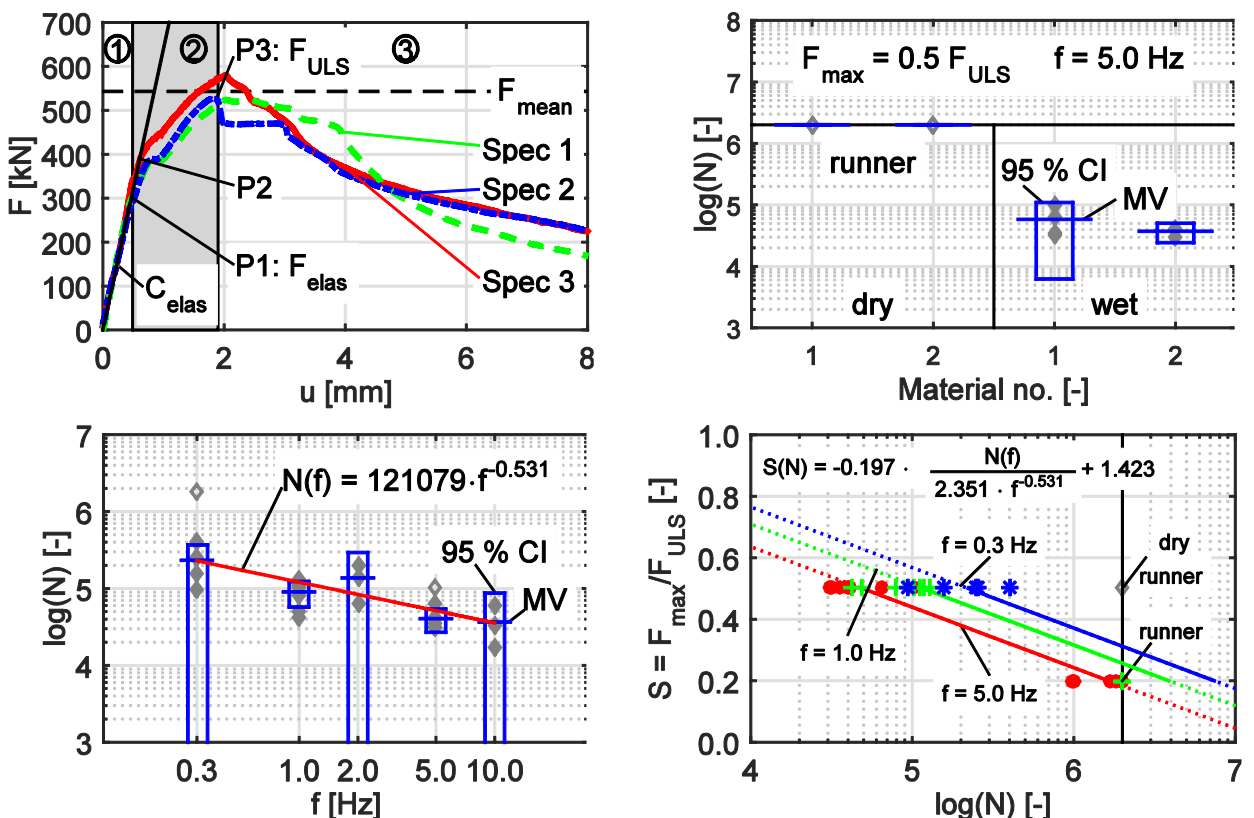


Figure 3: Force displacement behaviour of three specimen under quasi static compression (top left), number of endurable load cycles in different ambient conditions (AC) (top right), number of endurable load cycles for different loading frequencies (bottom, left) and loading frequency dependent S-N curve for small-scale specimens (bottom, right)

tests are conducted to investigate the influence of different loading frequencies. Figure 3, bottom left shows the resulting endurable load cycles for different loading frequencies. A reduction in the loading frequency causes an increase of endurable load cycles. This behaviour contradicts the observations made by Waagaard [6] for submerged reinforced concrete specimens and by Soerensen [7] for submerged grout material specimens. Both researchers noticed a reduction of endurable load cycles with a reduction of the loading frequency. Thus, the structural interaction between grout and steel influences damage mechanisms caused by the water. Schaumann et al. [8] derived a loading frequency dependent S-N curve for submerged small-scale specimens from the presented results (cf. Figure 3, bottom right).

During the submerged tests processes of grout material flushing were observed (cf. Figure 4, left). As a result the volume of the grout section reduces and the stiffness of the connection decreases. Subsequent to the tests, the specimens were opened to investigate the damaged grout section. Figure 4, right, shows the grout section of a specimen tested in dry and one tested in wet ambient conditions. Both specimens were tested with identical loading conditions. While for dry AC no effects of attrition were visible, the submerged specimen shows significant cracks due to transverse tensile stresses in the lower part, as well as vertical cracks in the upper part of the grout section.

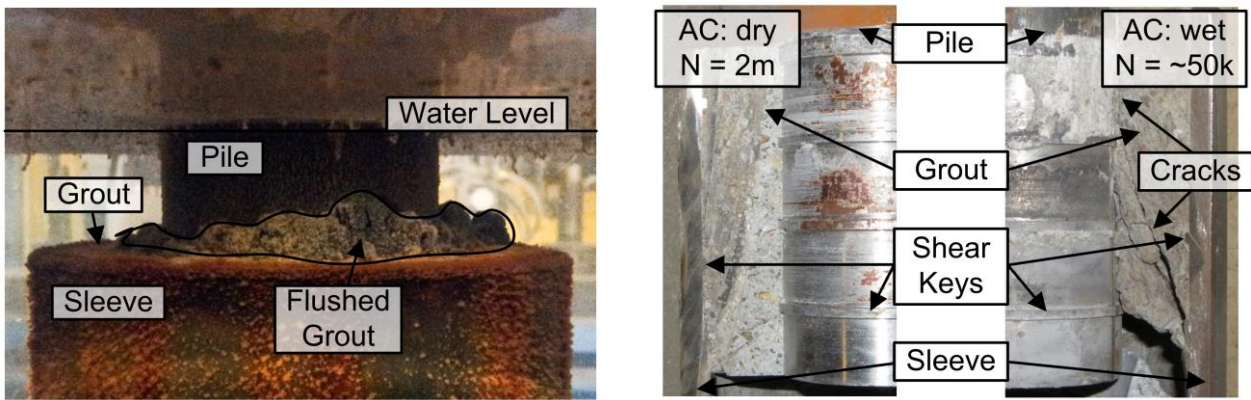


Figure 4: Flushed grout material on top of cyclically loaded submerged small-scale specimen (left) and grout section of opened specimens tested in dry (center) and wet (right) ambient conditions

Based on the presented results it can be suggested, that the water introduces three new damage mechanisms to the connections fatigue performance. The first process is initiated by loading the specimen. This leads to an opening of the contact interface between steel and grout. Thus, water invades the interface and alternating loads pump it through the connection. The water causes a hydro lubrication of the interface and reduces the friction between steel and grout (cf. [19]). The second process is introduced by the high local compressive loads in front of the shear keys. These loads cause a crushing of grout material, a process well known from specimens tested in dry AC (cf. [9]). But since water is pumped through the interface, the crushed material is spilled out of the connection, the grout volume reduced over time and therefore the specimen slips. And finally, pore water overpressure introduces micro cracks. These cracks become the starting point of the compression strut cracks observed in dry AC tests (cf. [10]). But in wet AC the compression strut cracks occur at lower load levels.

3 Large-scale tests

To evaluate the impact of large grout layer thicknesses to the load bearing behaviour and to the fatigue strength large-scale fatigue tests were performed at the Institute for Steel Construction in the testing frame IST of the Institute for Building Material Science, cf. Figure 5. The grout

layer geometries in jackets, like diameter to thickness ratio D_g/t_g , exceed current validity ranges of code recommendations by Norsok [11], ISO 19902 [12] and DNV [13], which originate from former experimental tests on grouted connections for oil and gas platforms for instance by Billington & Lewis [10]. Lotsberg et al. [14] performed cylindrical and box test specimens considering jacket and monopile dimensions to derivate fatigue design proposals, which are included as conservative design S-N curves in [13]. In contrast to these previous test specimens the herein presented specimens are equipped with two rather large grout annuli with $t_g \sim 80$ mm and 180 mm. The specimens are filled with the same grout materials used for the small-scale test specimens, which have a significantly higher compressive strength than formerly used cement slurries. The grouting was conducted in dry specimens to exclude influences of submerged grouting on the material performance. Prior to the experimental testing numerical calculations were used to characterize the fatigue strength of axially loaded grouted connections, cf. Schaumann et al. [15] and [16]. However, in the following the focus is set on the experimental test results of the test specimens TS01 - 04.

The large-scale test specimens TS01 - 04 were exposed to different load stages being characterized by initial axial alternating loads ($R = -1$) followed by axial pulsating compression loads ($R = \infty$). Since the precise moment of failure is unknown upfront and each specimen is a singleton, the loads were increased stepwise after reaching 100'000 load cycles at each load level, cf. [17] to find the moment of failure. To quantify the fatigue behaviour the test specimens were equipped with strain gauges and lasers to measure any strain developments and relative

Table 1: Validity ranges according to current standards [11], [12], [13] and test specimen dimensions acc. to Lotsberg et al. [14], acc. to Billington & Lewis [10] and own large-scale test specimens TS01 - 04.

Construction parameter	Validity range acc. to [11], [12], [13]	Large-scale test specimens TS01 - 04	Billington & Lewis [10]	Lotsberg et al. [14]
pile geometry	$20 \leq D_p/t_p \leq 40$ (60)*	$16 \leq D_p/t_p \leq 24$	$9.7 \leq D_p/t_p \leq 45$	$16 \leq D_p/t_p \leq 83$
sleeve geometry	$30 \leq D_s/t_s \leq 140$	$D_s/t_s = 41$	$18 \leq D_s/t_s \leq 140$	$40 \leq D_s/t_s \leq 100$
grout geometry	$10 \leq D_g/t_g \leq 45$	$4.2 \leq D_g/t_g \leq 9.5$	$6.5 \leq D_g/t_g \leq 26$	$29 \leq D_g/t_g \leq 44$
grout thickness	-	$80 \leq t_g \leq 185$ [mm]	$11 \leq t_g \leq 75$ [mm]	$18 \leq t_g \leq 100$ [mm]
grout strength	$f_{cu} \leq 80$ [MPa]	$90 < f_{cu} \leq 140$ [MPa]	$f_{cu} < 65$ [MPa]	$f_{cu} \leq 160$ [MPa]
shear key interlocking	$0.0 \leq h/s \leq 0.10$	$h/s = 0.06$	$0.0 \leq h/s \leq 0.04$	$0.0 \leq h/s \leq 0.06$
shear key distance	$D_p/s \leq 16$	$4 \leq D_p/s \leq 6$	$D_p/s \leq 16$	$D_p/s \leq 16$
radial stiffness	$K \leq 0.02$	$0.04 \leq K \leq 0.07$	$K \leq 0.04$	$K \leq 0.01$

* according to [13]

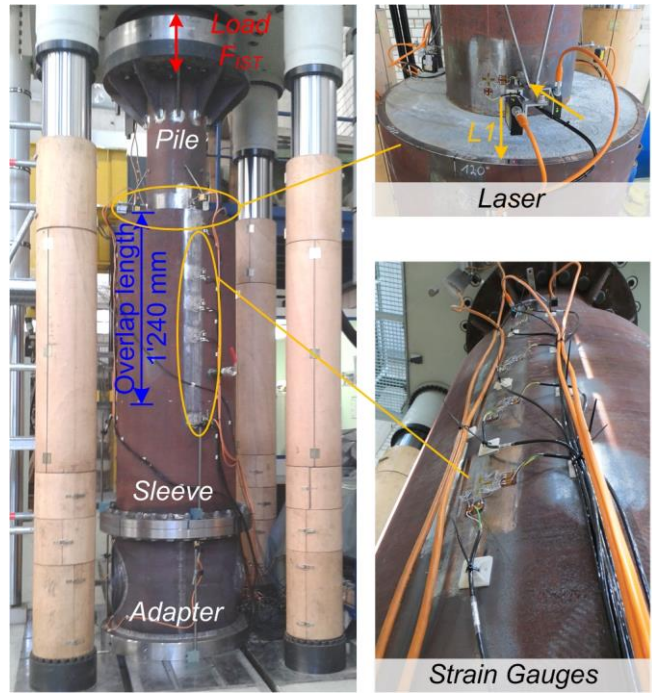


Figure 5: Large-scale grouted connection test specimen in testing frame (left) and corresponding measurements by laser (top right) and by strain gauges (bottom right)

The figure illustrates the experimental setup and measurement techniques used for the large-scale grouted connection test specimens. The left image shows the full specimen assembly within a hydraulic press frame. The top right image focuses on the upper section, showing a laser measurement point labeled L1. The bottom right image shows the lower section with strain gauge sensors attached to the pile and sleeve interface.

The figure provides a visual representation of the complex geometry of the grouted connection, including the pile, sleeve, adapter, and grout annuli. The strain gauges and laser measurement points are precisely located to capture the mechanical behavior and strain distributions during the fatigue test.

Table 1: Validity ranges according to current standards [11], [12], [13] and test specimen dimensions acc. to Lotsberg et al. [14], acc. to Billington & Lewis [10] and own large-scale test specimens TS01 - 04.

Construction parameter	Validity range acc. to [11], [12], [13]	Large-scale test specimens TS01 - 04	Billington & Lewis [10]	Lotsberg et al. [14]
pile geometry	$20 \leq D_p/t_p \leq 40$ (60)*	$16 \leq D_p/t_p \leq 24$	$9.7 \leq D_p/t_p \leq 45$	$16 \leq D_p/t_p \leq 83$
sleeve geometry	$30 \leq D_s/t_s \leq 140$	$D_s/t_s = 41$	$18 \leq D_s/t_s \leq 140$	$40 \leq D_s/t_s \leq 100$
grout geometry	$10 \leq D_g/t_g \leq 45$	$4.2 \leq D_g/t_g \leq 9.5$	$6.5 \leq D_g/t_g \leq 26$	$29 \leq D_g/t_g \leq 44$
grout thickness	-	$80 \leq t_g \leq 185$ [mm]	$11 \leq t_g \leq 75$ [mm]	$18 \leq t_g \leq 100$ [mm]
grout strength	$f_{cu} \leq 80$ [MPa]	$90 < f_{cu} \leq 140$ [MPa]	$f_{cu} < 65$ [MPa]	$f_{cu} \leq 160$ [MPa]
shear key interlocking	$0.0 \leq h/s \leq 0.10$	$h/s = 0.06$	$0.0 \leq h/s \leq 0.04$	$0.0 \leq h/s \leq 0.06$
shear key distance	$D_p/s \leq 16$	$4 \leq D_p/s \leq 6$	$D_p/s \leq 16$	$D_p/s \leq 16$
radial stiffness	$K \leq 0.02$	$0.04 \leq K \leq 0.07$	$K \leq 0.04$	$K \leq 0.01$

displacements occurring during testing, cf. Figure 5.

The initial test specimen behaviour is reflected by the load-displacement curve in Figure 6, left, showing the applied force F_{IST} and the relative displacement u_{IST} of the hydraulic cylinder. The test specimens with an odd number are realized with a large grout thickness representative for pre-piled jackets, whereby test specimens with even numbers represent grout layers used for post-piled tripods, cf. Figure 6, right. However, the initial load hysteresis at load stage LS01 with maximum loads of $F_{IST} = +/- 1'000$ kN indicates apart from a relatively linear-elastic behaviour that increasing grout thickness at TS01 and TS03 leads to reduced stiffness and increased displacements u_{IST} compared to TS02 and TS04, both having a smaller grout annulus. Comparing the load displacement values u_t of TS01 and TS03 for tensile loading reveals that the material impact seems to gain importance for an increasing grout layer thickness.

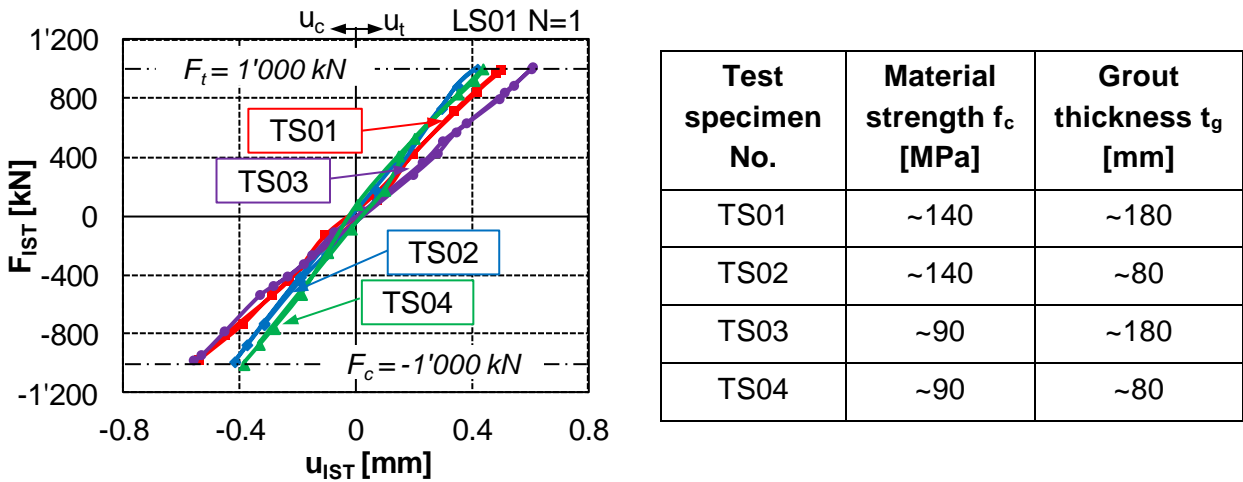


Figure 6: Load-displacement hysteresis of the test specimens TS01 - 04, summarized in the right Table, for the initial load cycle at load stage LS01 with $F = +/- 1'000$ kN.

The test specimen's fatigue behaviour at alternating loading is demonstrated for instance during load stage LS02 with $F = +/- 2$ MN in Figure 7 by representing the measured relative displacements of the connection at laser L1, cf. Figure 5 top right, over the applied number of load cycles N. The left diagram reveals relative displacements for the test specimens having a larger grout annulus, TS01 and TS03, and the right one depicts the results for the smaller grout annulus specimens, TS02 and TS04. Obviously the comparison of appearing relative displacements for the different grout layer thicknesses shows a significantly decreased stiffness with increasing grout annulus size. This complies to the initial load-displacement hysteresis. However, for TS01 and TS03 a progressive rise of relative displacements is documented by the lasers over the applied number of load cycles. By contrast the relative displacements at TS02 and TS04 develop more constant showing no significant stiffness reduction. With regard to the different filling materials the previous assumption of increased material impact with increasing grout thickness is confirmed by Figure 7, as the relative displacements at TS03 are significantly larger than at TS01. Comparing tensile and compression induced relative displacements reflect that the tensile capacity is smaller than the compression based capacity as corresponding relative displacements are larger than compression induced displacements. This is caused by the construction of the test specimens having 4 shear key pairs, compression struts respectively, that can be activated at tensile loading and 5 shear key pairs, compression struts respectively, that can be activated at compression loading.

From the presented test results it can be concluded that the grout layer thickness permanently influences the fatigue strength of grouted connections. Even though the impact of the material strength is an inferior impact factor compared to the grout thickness and remaining geometrical dimensions, its impact rises with increasing grout layer thickness. Apart from these results, in [17] arising compression struts, failure modes and damage patterns are discussed, reflecting a compression strut change depending on the angle between opposed shear keys and depending on the grout layer thickness. Further investigations and test results are presented, discussed and evaluated in [18].

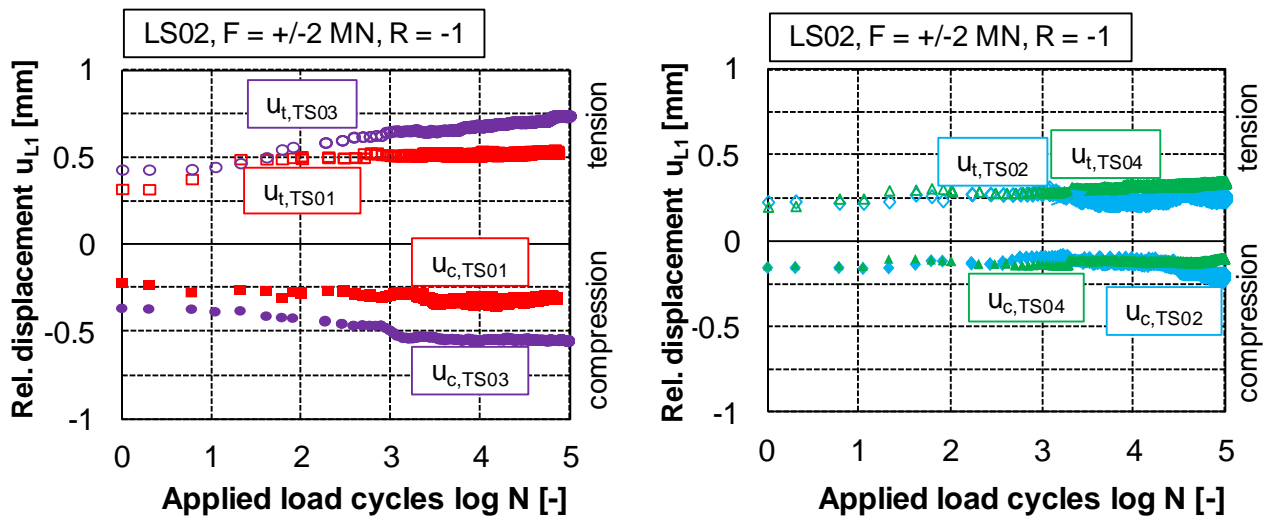


Figure 7: Development of the relative displacements u_{L1} at laser L1 in load stage LS02 for maximum load of $F = +/- 2 \text{ MN}$ for TS01 and TS03 (left) and TS02 and TS04 (right)

4 Conclusions

In this paper, results of small and large scale specimen tests of axially loaded grouted connections are presented. The small scale specimen fatigue tests show a significant impact of water on the connection's fatigue behaviour. As mentioned, the small scale specimens are not real to scale and therefore, the presented results cannot be directly transferred to real connections.

Large-scale fatigue test results have shown that differing grout thicknesses have a permanent impact to the fatigue strength, especially considering alternating load stages. Apart from this, the material impact increases with increasing grout layer thickness. However, the test results achieved by small-scale test results will be complemented by future submerged large-scale fatigue tests of grouted connections.

5 Acknowledgement

The presented experimental tests and results are achieved within the research project 'Grouted Joints for Offshore Wind Energy Converters under reversed axial loadings and upscaled thicknesses – GROWup' (BMWi, funding sign: 0325290). The authors thank the German Federal Ministry for Economic Affairs and Energy for funding and all accompanying industrial partners (DNV GL, Senvion SE, Siemens Wind Power, Wilke & Schiele Consulting GmbH, Bilfinger Marine & Offshore Systems GmbH) for their expert advice. Moreover, the authors thank the material manufacturers Densit and BASF. A final acknowledgment goes to the Institute for Building Materials Science for the cooperative partnership.

6 References

- [1] Bundesregierung (2013): "Koalitionsvertrag zwischen CDU, CSU und SPD - 18. Legislaturperiode". www.tagesschau.de/inland/koalitionsvertrag152.pdf.
- [2] BSH D-OWT (2007): "Standard - Design of Offshore Wind Turbines". German Maritime and Hydrographic Agency.
- [3] Schaumann P. and Wilke F. (2006): "Fatigue Assessment of Support Structures of OWEC Systems", Annual Report 2005, pp. 36–39, Hannover, Germany.
- [4] Schaumann P., Bechtel A. and Lochte-Holtgreven S. (2010): "Fatigue Performance of Grouted Joints for Offshore Wind Energy Converters in Deeper Waters", Proceedings of the 20th ISOPE, pp. 672–679, Beijing, China.
- [5] Schaumann P., and Raba A. (2015): "Systematic Testing of the Fatigue Performance of Submerged Small-Scale Grouted Joints". Proceedings of the 34th OMAE, St. John's, Newfoundland, Canada.
- [6] Waagaard K. (1986): "Experimental Investigation on the Fatigue Strength of Offshore Concrete Structures". Proceedings of the 9th Annual Energy Technology Conference, pp. S. 73-81, New Orleans, Louisiana, USA.
- [7] Soerensen E. V. (2011): "Fatigue Life of High Performance Grout in Dry and Wet Environment for Wing Turbine Grouted Connections". Proceedings of the EWEA Offshore, Amsterdam, Netherlands.
- [8] Schaumann P. and Raba A. (2015): "Influence Of The Loading Frequency On The Fatigue Performance Of Submerged Small-Scale Grouted Joints". Proceedings of the 12th DEWEK, Bremen, Germany.
- [9] Krahl N. W. and Karsan D. I. (1985): "Axial Strength of Grouted Pile-to-Sleeve Connections". Journal of Structural Engineering, 111(4), pp. 889–905.
- [10] Billington C. J. and Lewis H. G. (1978): "The Strength of Large Diameter Grouted Connections", Proceedings of the OTC, pp. 291–301, Houston, Texas, USA.
- [11] Norsok Standard N-004 (2013): "Design of steel structures", Rev. 3, Standards Norway, Lysaker, Norway.
- [12] DIN EN ISO 19902 (2014): "Petroleum and natural gas industries - Fixed steel offshore structures", German version, Deutsches Institut für Normung e.V., Beuth Verlag, Berlin.
- [13] DNV-OS-J101 (2014): "Design of Offshore Wind Turbines Structures", Det Norske Veritas
- [14] Lotsberg, S. Bertnes, H., Lervik, A. (2013): "Capacity of Cylindrical Shaped Grouted Connection with Shear Keys - Background Report", Report No. 2011-1415, Rev. No. 09, Det Norske Veritas, Høvik, Norway (unpublished).
- [15] Schaumann, P., Bechtel, A., Lochte-Holtgreven, S. (2010): "Fatigue design for axially loaded grouted connections of offshore wind turbine support structures in deeper waters", in Proceedings of the Earth & Space Conference, pp. 2047 - 2054, Hawaii, USA.
- [16] Schaumann, P., Bechtel, A., Lochte-Holtgreven, S. (2013): "Grouted Joints for Offshore Wind Turbines Jackets under Full Reversal Axially Loading Conditions", in Proceedings of the 23rd ISOPE, pp. 173 - 180, Anchorage, Alaska, USA.
- [17] Schaumann, P., Raba, A., Bechtel, A. (2014): "Experimental Fatigue Tests on axially loaded grouted joints", Proceedings of the IWEC, Hannover, Germany.
- [18] Bechtel, A. (2016): "Fatigue Behaviour of Axially Loaded Grouted Connections in Offshore Support Structures", PhD-Thesis, Institute for Steel Construction, Leibniz University Hannover, Germany (in preparation).
- [19] Schaumann, P., Raba, A., Bechtel, A. (2013): "Impact of Contact Interface Conditions on the Axial Load Bearing Capacity of Grouted Connections" in Proceedings of the European Wind Energy Association Conference EWEA 2013. Vienna, Austria.